Molecular Biology Reports (2024) 51:530
https://doi.org/10.1007/s11033-024-09406-8

ORIGINAL ARTICLE

SIRT1 and ZNF350 as novel biomarkers for osteoporosis: a bioinformatics analysis and experimental validation

Naiqiang Zhu[1,2] · Jingyi Hou[5] · Jingyuan Si[3] · Ning Yang[4] · Bin Chen[2] · Xu Wei[1] · Liguo Zhu[1]

Received: 10 September 2023 / Accepted: 29 February 2024

Abstract

Background Osteoporosis (OP) is characterized by bone mass decrease and bone tissue microarchitectural deterioration in bone tissue. This study identified potential biomarkers for early diagnosis of OP and elucidated the mechanism of OP.

Methods Gene expression profiles were downloaded from Gene Expression Omnibus (GEO) for the GSE56814 dataset. A gene co-expression network was constructed using weighted gene co-expression network analysis (WGCNA) to identify key modules associated with healthy and OP samples. Functional enrichment analysis was conducted using the R clusterProfiler package for modules to construct the transcriptional regulatory factor networks. We used the "ggpubr" package in R to screen for differentially expressed genes between the two samples. Gene set variation analysis (GSVA) was employed to further validate hub gene expression levels between normal and OP samples using RT-PCR and immunofluorescence to evaluate the potential biological changes in various samples.

Results There was a distinction between the normal and OP conditions based on the preserved significant module. A total of 100 genes with the highest MM scores were considered key genes. Functional enrichment analysis suggested that the top 10 biological processes, cellular component and molecular functions were enriched. The Toll-like receptor signaling pathway, TNF signaling pathway, PI3K-Akt signaling pathway, osteoclast differentiation, JAK-STAT signaling pathway, and chemokine signaling pathway were identified by Kyoto Encyclopedia of Genes and Genomes pathway analysis. SIRT1 and ZNF350 were identified by Wilcoxon algorithm as hub differentially expressed transcriptional regulatory factors that promote OP progression by affecting oxidative phosphorylation, apoptosis, PI3K-Akt-mTOR signaling, and p53 pathway. According to RT-PCR and immunostaining results, SIRT1 and ZNF350 levels were significantly higher in OP samples than in normal samples.

Conclusion SIRT1 and ZNF350 are important transcriptional regulatory factors for the pathogenesis of OP and may be novel biomarkers for OP treatment.

Keywords Osteoporosis · Co-expression · WGCNA · Bioinformatics analyses · Biomarkers

Naiqiang Zhu and Jingyi Hou equally contributed to this work.

✉ Xu Wei
weixu.007@163.com

✉ Liguo Zhu
tcmspine@163.com

[1] Wangjing Hospital, China Academy of Chinese Medical Sciences, Beijing 100102, China

[2] Department of Minimally Invasive Spinal Surgery, The Affiliated Hospital of Chengde Medical University, Chengde 067000, China

[3] South Operation Department, The Affiliated Hospital of Chengde Medical University, Chengde 067000, China

[4] Central Laboratory, The Affiliated Hospital of Chengde Medical University, Chengde 067000, China

[5] Chengde Medical University, Chengde 067000, China

Published online: 18 April 2024

Introduction

Osteoporosis (OP) is a systemic metabolic skeletal disease characterized by osteopenia and disruption of bone microstructure, resulting in increased bone fragility and fracture incidence [1]. With the aging of the population and the widespread use of glucocorticoids, OP has become an "invisible killer" [2].With the global population over 60 years of age expected to reach two billion by 2050, the incidence of OP is expected to increase rapidly and have a major impact on older adults' health and quality of life, especially postmenopausal females [3, 4]. In recent years, progress has been made in the research on the occurrence and pathogenesis of OP using molecular biology, cell biology, and other methods, mainly focusing on the Wnt/β-catenin [5, 6] and JAK/STAT signaling pathways [7, 8]. However, focusing only on a single gene or several genes from a local perspective can no longer satisfy this highly complex regulatory research. Based on the overall regulatory network, genes in OP are specifically expressed and closely related to regulatory factors [9], that are important in the occurrence and development of OP. Therefore, identify biomarkers for the occurrence and progression of OP is important for clinical diagnosis. Although the amount of biological data has increased exponentially with the rapid development of high-throughput technologies, most current informatics research has focused on studying differential gene expression, ignoring the possible correlations between genes and expression types. Weighted Gene Co-expression Network Analysis (WGCNA), a biotechnology based on scale-free networks, visually displays the interrelationships between various parts of biological systems and more accurately displays the characteristics of biological systems. This provides an important method for systematically studying diseases' physiological and pathological processes [10]. WGCNA has been used in the genetic analysis of diseases like breast cancer [11], diabetes mellitus [12], Alzheimer's disease [13], and coronary atherosclerotic heart disease [14], confirming that these modules and key genes play key roles in disease progression.

This study's analysis of the GEO GSE56814 dataset revealed OP-associated hub transcriptional regulators. Bioinformatics analysis revealed the potential functions of OP-associated hub genes, and molecular biology experiments were performed to validate new biomarkers associated with OP progression (Fig. 1).

Methods

Materials

Three normal and three osteoporotic bone tissues were collected from The Affiliated Hospital of Chengde Medical University (Chengde, Hebei, China) from 2020 to 2023, and are listed in Supplementary Table 1, which was approved by the Ethics Committee of The Affiliated Hospital of Chengde Medical University (2022.06.16/ No. CYFYLL2020240). The samples were immediately stored in -80°C refrigerator for further experimental validation. The TRIzol reagent was procured from Invitrogen Co., Ltd. DEPC water was acquired from Soleibao Technology Co., Ltd. (Beijing, China). The HiFi-ScriptTM Reverse Transcription Kit was purchased from Kangwei Reagent Co., Ltd., and TB Green Premix Ex Taq II was obtained from Tiangen Biochemical Technology Co., Ltd. The antibodies SIRT1 and ZNF350, as well as GAPDH, were procured from Bioss Biological Technology Co., Ltd (Beijing, China, NO. BS-0921R and BS-1630R) and Gene Tex Biological Technology Co., Ltd (Beijing, China, NO. TEX112053 and GTX100118). Cy3-labeled Goat Anti-Rabbit IgG was obtained from Zhongshan Golden Bridge Biotechnology Co., Ltd. (Beijing, China). Chromatographic-grade solvents (chloroform, ethanol, xylene, and isopropanol) were acquired from Tianjin Yongda Chemical Reagent Co. Ltd. (Tianjin, China).

Datasets and samples

The GSE56814 dataset was downloaded from the GEO database using GeoQuery package [15]. In the GSE56814 dataset, hip bone mineral density (BMD) was measured using a Hologic 4500-W dual-energy X-ray absorptiometer (DXA) scanner (Hologic Corp., Waltham, MA), and the diagnostic criteria for high and low BMD were defined based on the top and bottom 30% of BMD values within our population. This dataset obtained total RNA from 60 milliliters of peripheral blood of 31 patients with OP and 42 healthy individuals. Subsequently, mRNA expression levels were quantified using the GeneChip Human Exon 1.0 ST Array (Affymetrix, Santa Clara, CA) in accordance with the manufacturer's protocol. For WGCNA, we utilized annotation information from the GPL5175 biochip platform to match gene probes with their corresponding gene names.

Analyses of module stability and weighted co-expression networks

Based on the protocol of the WGCNA package in the R language, weighted co-expression networks (Healthy and OP) were constructed [16]. Paired Pearson correlations were

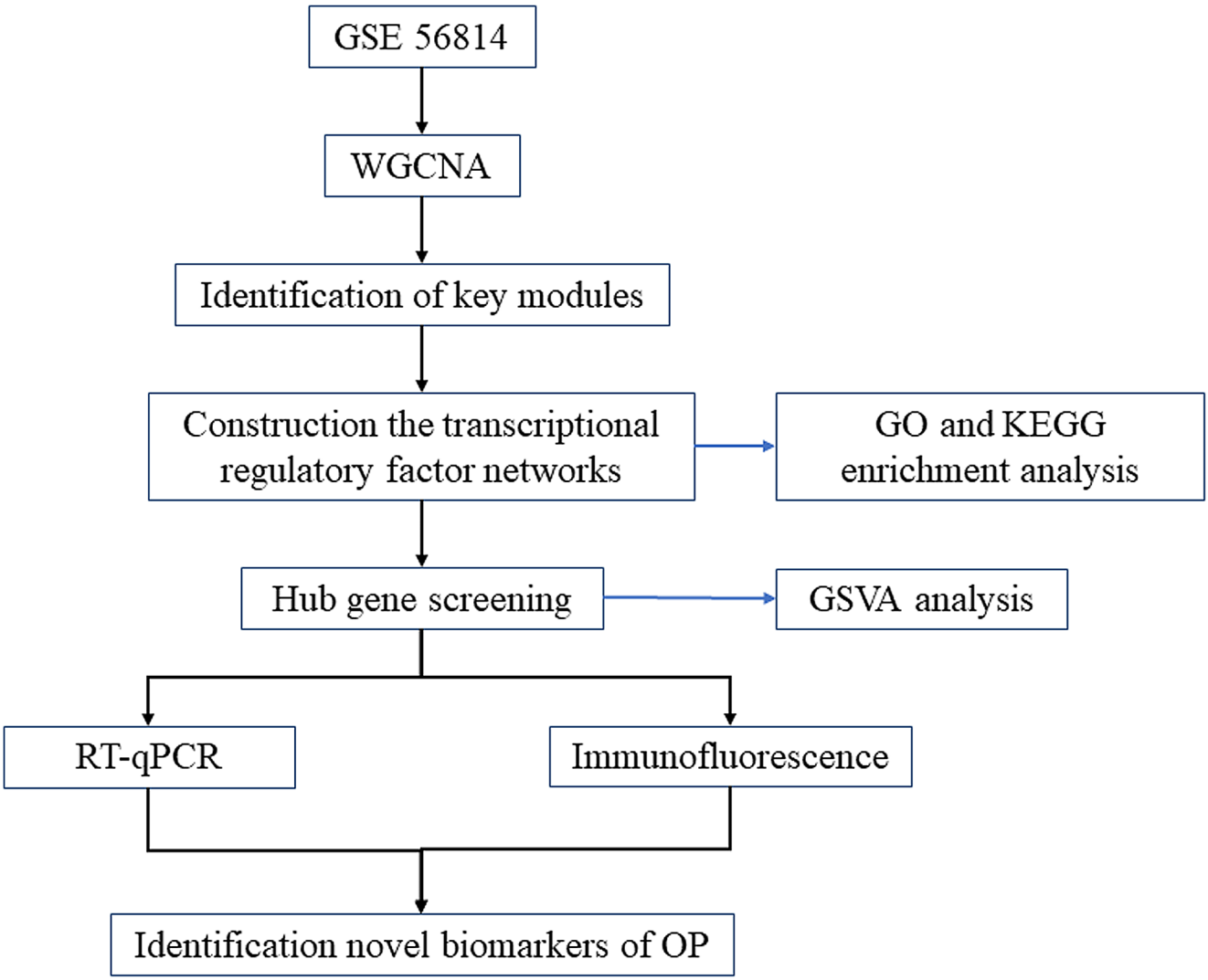

Fig. 1 Complete flow diagram of the study

applied to evaluate the weighted co-expression relationships among subjects in the adjacency matrix. An appropriate power value was determined if the degree of independence was 0.9. Gene modules were identified using a topological overlap matrix (TOM)-based hierarchical clustering approach based on dissimilarity measures (1-TOM). We then performed a 50-fold permutation test to classify modules not conserved in the normal and OP co-expression networks according to the module conservation function of the WGCNA package [17]. Modular genes are highly interconnected intra-module genes whose corresponding modules have the highest modular association (MM) values. We calculated the MM of each gene using the WGCNA function signedME, and considered the 100 genes with the highest MM values as key genes.

Construction of transcriptional regulatory factor network and functional enrichment analysis

The TRRUST Database (https://www.grnpediöttrust) [18, 19] records the regulatory relationships of transcription factors, which contain the targets corresponding to transcription factors and the regulatory relationships between transcription factors, describing a comprehensive transcriptional factor regulatory network. In this study, modular genes were mapped into the transcription factor regulatory network, and a modular gene-transcription factor regulatory relationship was obtained, which was visualized using the Cytoscape platform. We then used the ClusterProfiler package in R [20] to annotate genes associated with transcription factors and comprehensively studied the functional relevance of hub genes. Functional classification was assessed using Gene Ontology (GO) and the Kyoto Encyclopedia of

Genes and Genomes (KEGG), and significance was set at $P < 0.05$ and $q < 0.1$.

Hub genes screening

After extracting the expression of each gene in the Transcriptional Regulatory Factor Network, we applied the Wilcoxon algorithm to screen hub differentially expressed genes in normal samples and OP samples. In order to visualize the results, we used the "ggpubr" package in R to draw violin plots. Statistical significance was set at $P < 0.05$.

Gene set variation analysis (GSVA)

GSVA is a nonparametric, unsupervised method for assessing gene pool enrichment that converts changes at the gene level to changes at the signaling pathway level. The biological functions of the samples were evaluated [21]. In this study, we obtained a set of genes from the Molecular Signature Database (version 7.0). We comprehensively evaluated the key genes using the GSVA package in R (http://www.bioconductor.org/gsva) to assess possible changes in biological functions between different samples.

Reverse-transcription quantitative polymerase chain reaction (RT-qPCR)

Total RNA of bone tissues obtained from the Chengde Medical College's Affiliated Hospital in Chengde was isolated using a UNIQ-10 column TRIzol total RNA extraction kit, following the manufacturer's instructions. cDNA was generated using the HiFi-ScriptTM Reverse Transcription Kit at 37°C for 15 min, 85°C for 5 s, and 4°C in storage. PCR amplification was performed using TB Green Premix Ex Taq II. The primers used in this experiment were GAPDH, SIRT1, and ZNF350 (Homo sapiens; Supplementary Table 2). Each sample was tested in triplicate, and the relative expression of mRNA was calculated using the $2^{(-\triangle\triangle C_T)}$ method.

Immunofluorescence

Immunofluorescence analysis was performed as previously described [22]. Normal and surgical bone specimens were fixed in citric acid for 10 min aspirated, and infiltrated with 3% H_2O_2 for 20 min. Primary antibodies were applied overnight (SIRT1, 1:80; ZNF350, 1:120), followed by Cy3-conjugated goat anti-rabbit IgG for 20 min and DAPI for 20 min.

Statistical analysis

Data were analyzed using OriginPro8.0 software (USA), and expressed as mean ± standard error. One-way analysis of variance was used to analyze and compare the means of the different groups. P values < 0.05 were considered statistically significant.

Result

Identification of WGCNA modules

The original GSE56814 dataset was extracted from the GEO database, and R was used to perform background correction and normalization preprocessing on the original data. The Hclust function was used to remove batch effects, and the samples were randomly distributed to form a dendrogram. We selected power values 14 and 8 (the lowest power of the scale-free topology fitting index was 0.9) to generate OP and normal hierarchical clustering trees, respectively (Supplementary Fig. 2A-B). Normal samples were analyzed using WGCNA, and 15 modules were identified. The normal samples co-expression network modules were mapped to the disease sample network to evaluate the recurrence of module characteristics (Fig. 2A-B). To verify the stability of the identifier module, we used the module preservation function to calculate the preserved size of the module (Fig. 2C-D). The cyan module was retained with a lower degree of preservation (median rank = 2.0, Z-summary = 9.6), indicating that normal and OP states can be identified. The MM scores were calculated based on the WGCNA signed KME function, and the top 100 genes with the highest MM scores were considered key genes.

Construction of transcriptional regulatory factor network and functional enrichment analysis

Key genes were imported into the TRRUST database to create transcriptional regulatory factors and key gene networks. The network consisted of 21 transcriptional regulatory factor, 48 key gene nodes and 79 interaction edges (Fig. 3). The top 10 biological processes were enriched, including type I interferon signaling pathway, transcription, DNA-templating, transcription from RNA polymerase II promoter, positive regulation of type I interferon production, positive regulation of transcription, and negative regulation of transcription (Fig. 4A). The transcription factor complex, nucleus, nucleoplasm, nuclear matrix, nuclear chromatin, and cytoplasm were related to the cellular component (Fig. 4B). The top 10 molecular functions, including transcription regulatory region DNA binding, transcription

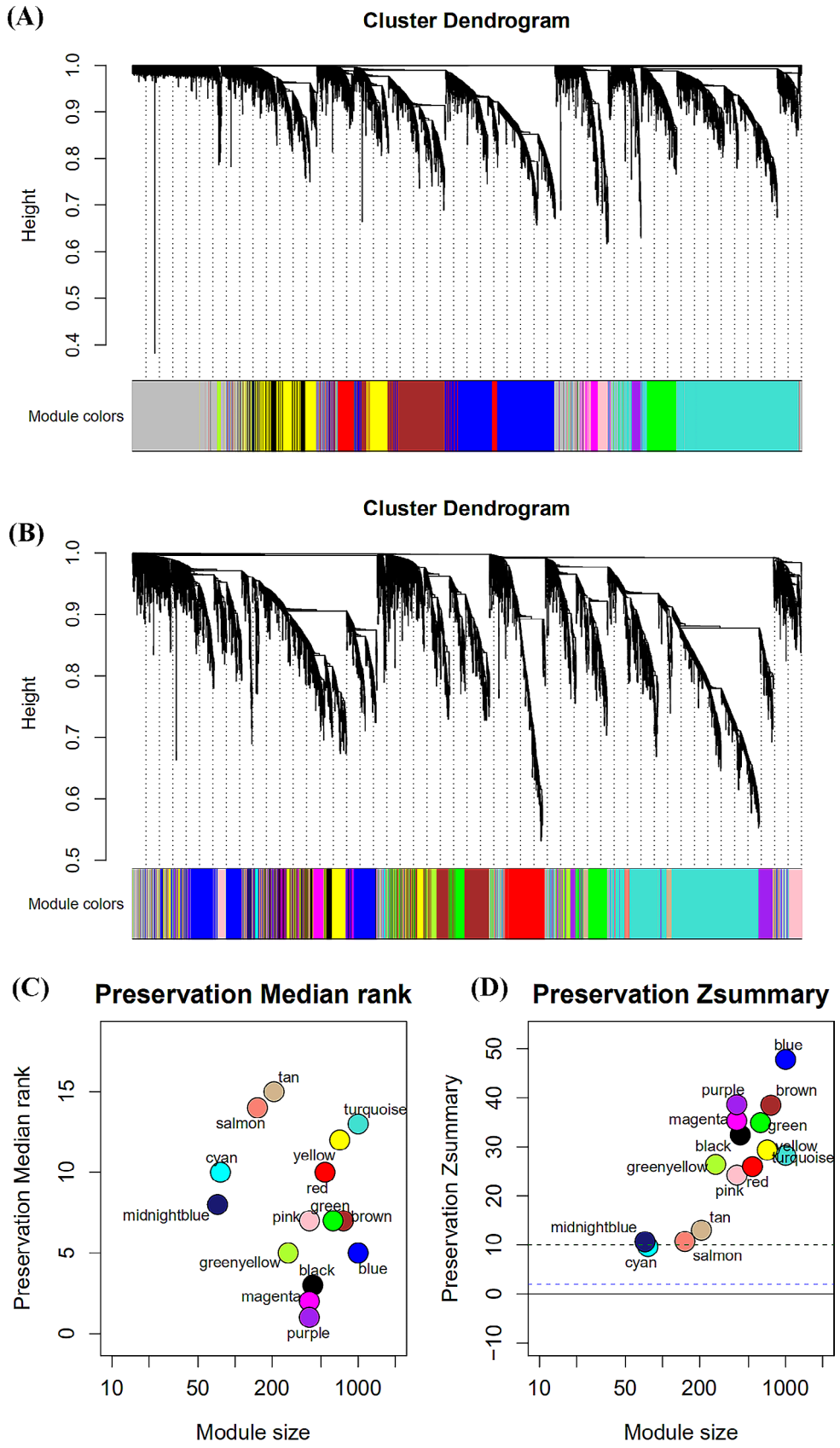

Fig. 2 Clustering dendrograms and the characterization of gene modules identified by WGCNA. (**A**) OP samples; (**B**) normal samples; (**C**) module preservation median rank; and (**D**) Z-summary score

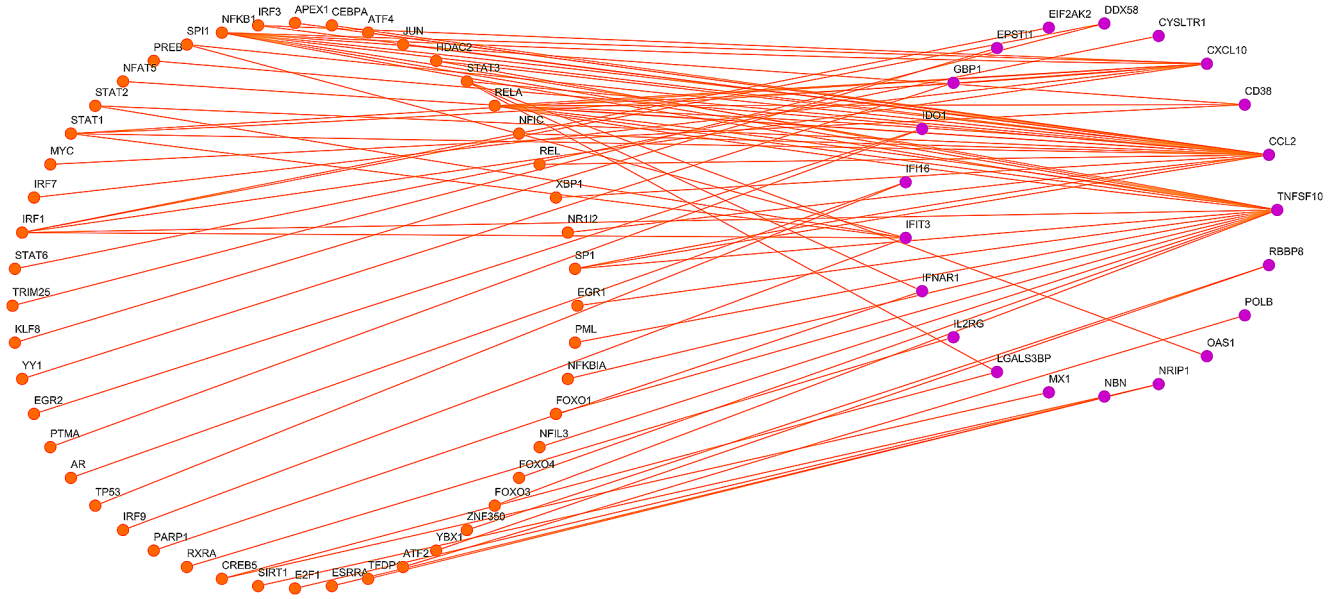

Fig. 3 Transcriptional regulatory factor -key genes network. Orange nodes represent transcriptional regulatory factor, and purple nodes represent key genes

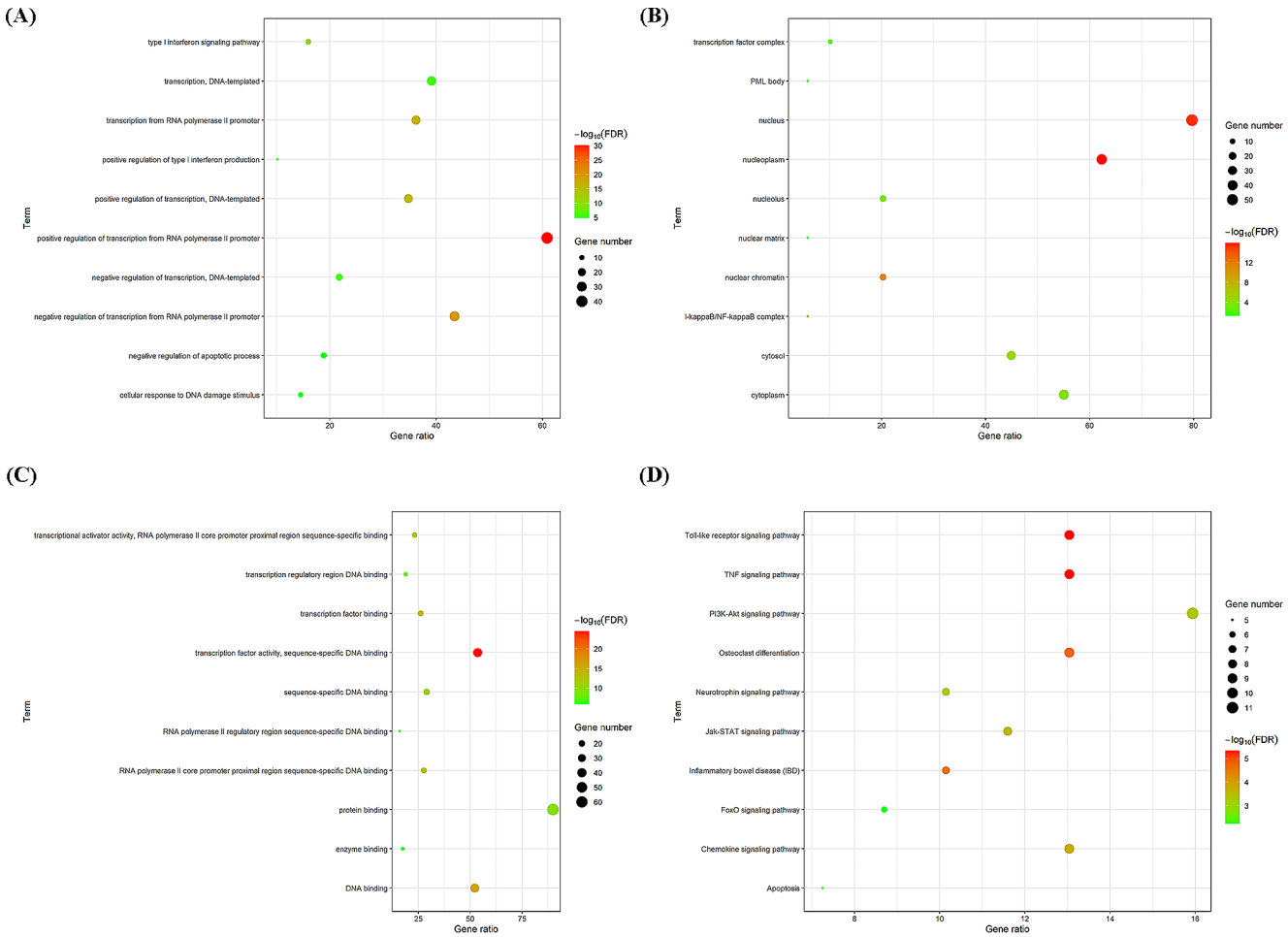

Fig. 4 Functional enrichment analysis of targets identified in the transcriptional regulatory factor-gene network. (**A**) Biological process analysis; (**B**) cellular component analysis; (**C**) molecular function analysis; and (**D**) KEGG pathway analysis

factor binding, protein binding, enzyme binding, DNA binding, and RNA polymerase II core promoter proximal region sequence-specific DNA binding, were identified (Fig. 4C). Regarding the KEGG pathway analysis (Fig. 4D), it was apparent that the targets mostly participated in the Toll-like receptor, TNF, PI3K-Akt, Osteoclast differentiation, JAK-STAT, and Chemokine signaling pathway.

Hub transcriptional regulatory factors screening and analysis

The plot in Fig. 5 shows the expression of differentially expressed transcriptional regulatory factors in normal and OP samples based on Wilcoxon algorithm, namely SIRT1, and ZNF350. A panel of 50 hallmark genes was screened in the normal and OP samples using GSVA to identify important signaling pathways (Fig. 6A); 31 significantly expressed hallmark gene sets were identified by GSVA in the samples with high expression of SIRT1. IL6 Jak Stat3 signaling, apoptosis, and PI3K-Akt-mTOR signaling were significantly differentially expressed in different expression groups of SIRT1. Additionally, PI3K-Akt-mTOR, oxidative phosphorylation, P53 pathway, apoptosis, and hypoxia were significantly differentially expressed in the different expression groups of ZNF350 (Fig. 6B), suggesting SIRT1 and ZNF350 promoted the progression of OP by affecting oxidative phosphorylation, apoptosis, PI3K-Akt-mTOR signaling, and p53 pathway.

Experimental validation

Hub genes in normal ($n=3$) and OP ($n=3$) samples were verified using RT-qPCR. The hub gene expression levels (SIRT1 and ZNF350) in normal and OP samples were as follows: 0.96 ± 0.05, 2.13 ± 0.19; 0.99 ± 0.90, 3.03 ± 0.54, respectively, indicating that the mRNA expression of hub gene detected in OP samples was significantly or extremely significantly increased compared with normal samples ($P < 0.05$ or, $P < 0.01$) (Fig. 7). Furthermore, we confirmed the differential expression of hub genes in the normal and OP samples using immunofluorescence. The immunostaining intensities of SIRT1 and ZNF350 were higher in the OP samples than in the normal samples (Fig. 8).

Discussion

OP, a systemic bone metabolic disease with a complex pathogenesis, affects the quality of life and causes serious clinical consequences and social burden; however its specific pathogenesis has not yet been fully clarified [23]. This study, employed bioinformatics analysis to screen OP transcriptional regulatory biomarkers and validate the molecular biology experiments. WGCNA was used to calculate the co-expression relationships between molecules in a network, identify hub genes in modules, and gain insight into the expression profiles associated with hub genes and functional gene connections. This study used GSE56814 expression profiles comprising 73 blood samples from 31 patients with OP and 42 healthy controls. The WGCNA algorithm was used to filter the key modules and calculate the conservative degree of the modules (Fig. 2), where the lower preservation cyan module can distinguish normal and OP networks based on normal and disease samples; therefor, the cyan module was selected as the key module for the following analysis. The top 100 genes with the highest MM scores were mapped to the TRRUST database to construct the transcriptional factor regulatory network. Targets

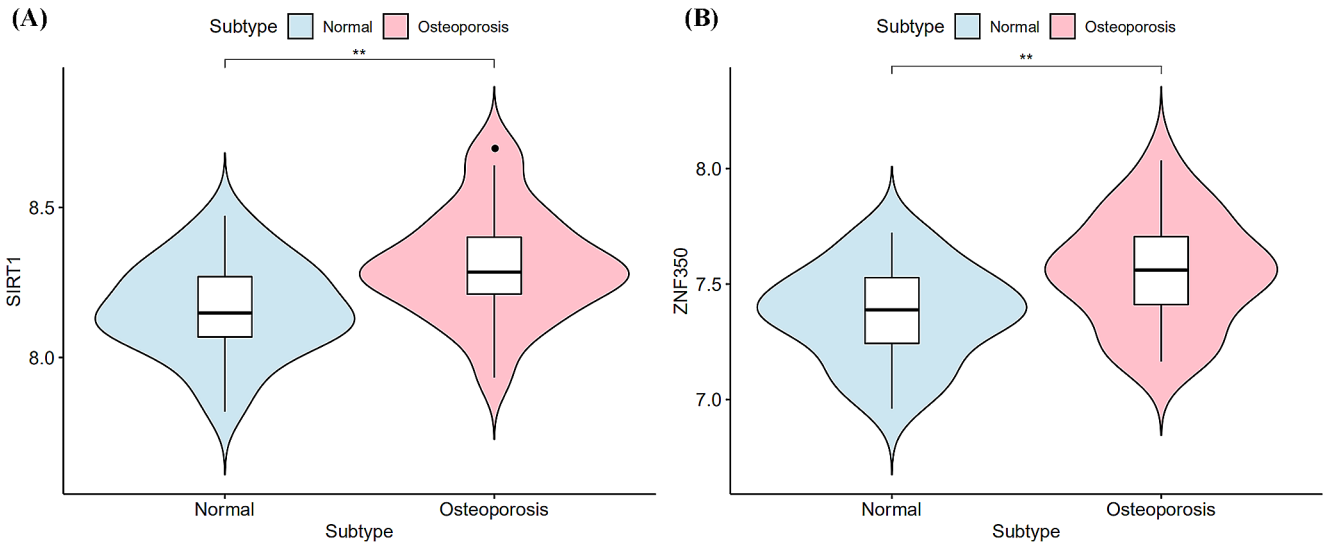

Fig. 5 The expression levels of the hub differentially expressed genes in normal and OP samples. (**A**) SIRT1 and (**B**) ZNF350

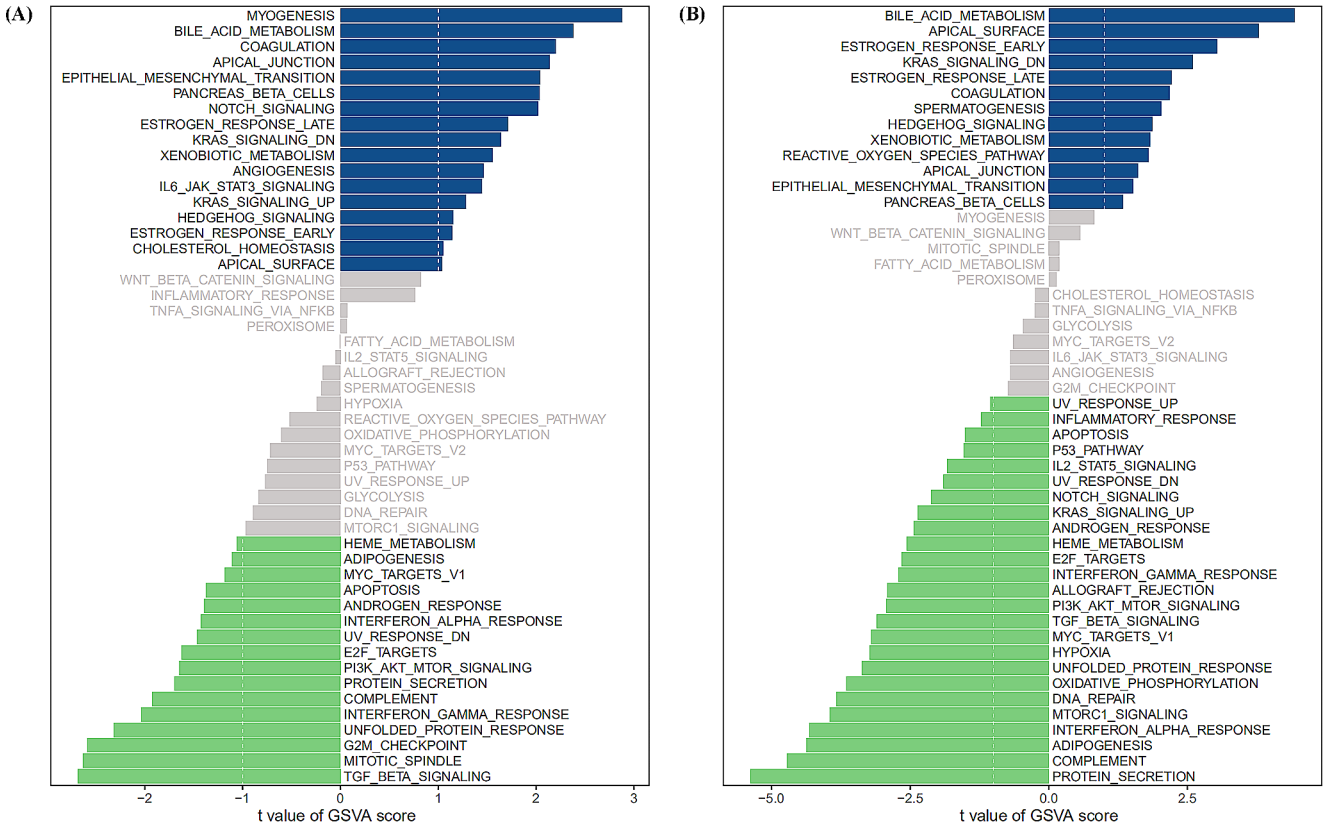

Fig. 6 GSVA analysis showing the activated hallmark pathways. (**A**) SIRT1 and (**B**) ZNF350

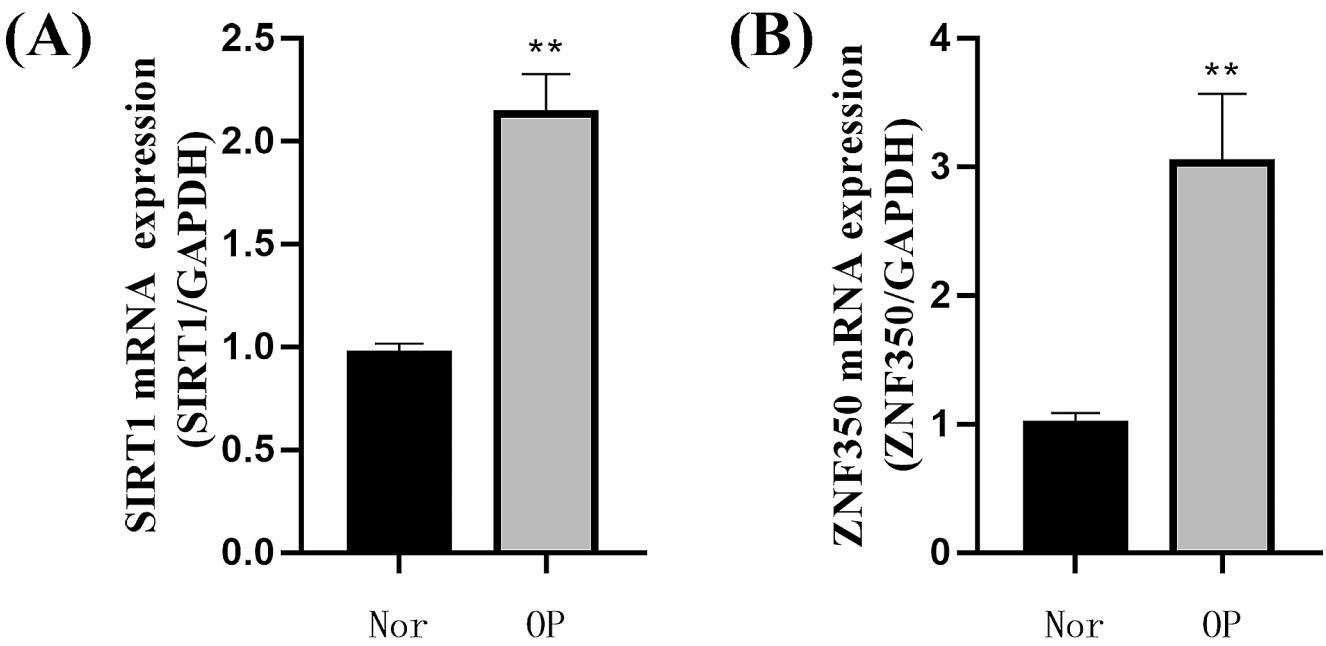

Fig. 7 Hub gene mRNA expression levels in normal and OP samples. (**A**) SIRT1 and (**B**) ZNF350. Data are presented as the mean ± SD ($n = 3$). * $P < 0.05$ and ** $P < 0.01$

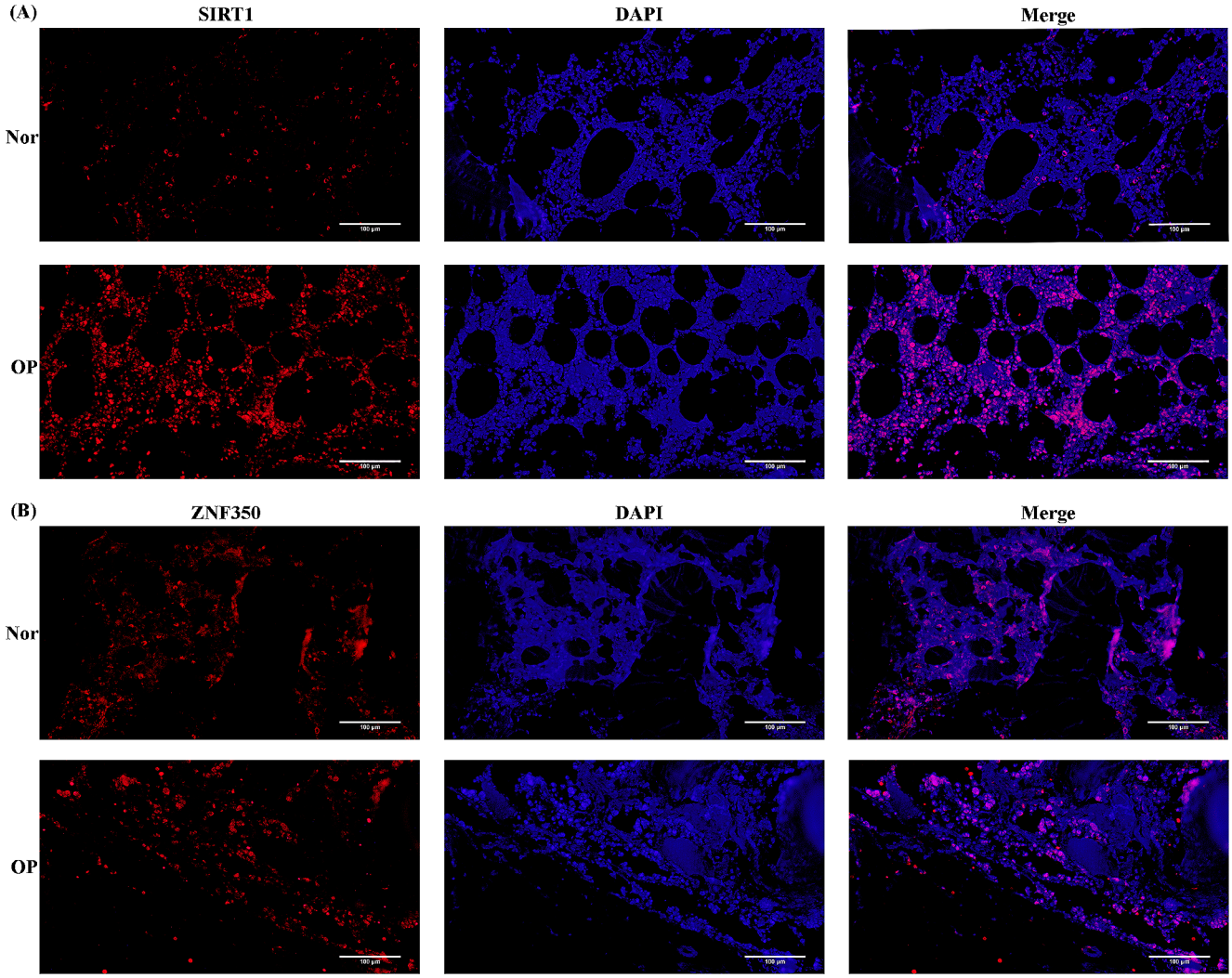

Fig. 8 Immunofluorescence staining of SIRT1 and ZNF350. (**A**) SIRT1 and (**B**) ZNF350. The red immunofluorescence in the pictures represent SIRT1 or ZNF350. Cell nuclei were counterstained with DAPI

involved in the transcriptional factor-gene regulatory network were enriched in the Toll-like receptor, TNF, PI3K-Akt, JAK-STAT and osteoclast differentiation signaling pathway. The PI3K-Akt signaling pathway is critical in differentiating skeletal cells such as osteoblasts, chondrocytes, myoblasts and adipocytes [24–26]. Xi et al. studied a rat OP model and a cultured osteoblast model. They showed that the PI3K/Akt signaling pathway suppresses OP by promoting osteoblast proliferation and differentiation and enhancing bone formation [27]. Osteoclast differentiation and activation have been elucidated through relevant biological assays of a family of proteins known as the tumor necrosis factor receptor (TNFR)/TNF-like proteins. This family includes osteoprotegerin, receptor activator of nuclear factor (NF)-κB (RANK), and the RANK ligand (RANKL) [28]. Cao et al. investigated the underlying mechanism of TRPV4 expression in osteoclast differentiation using M-CSF and RANKL-induced RAW264.7 macrophage cells [29]. They found that the downregulation of TRPV4 probably inhibits autophagy in osteoclast differentiation, thereby inhibiting OP. Yin et al. believed that glycyrrhizic acid (Gly) could inhibit NF-κB, ERK, and JUK signaling pathways in vitro, strongly inhibit osteoclast differentiation and bone resorption, and has a bone-protective effect on OVX mice [30]. The JAK-STAT signaling pathway was primarily recognized as a receptor-activated pathway in response to interferon (IFN)-γ and interleukin 6 (IL-6) cytokine family [31], and it is critical for cytokine effects on osteoblast proliferation and differentiation. Xu et al. suggested that fibroblast growth factor 23 (FGF23) is involved in bone and cartilage metabolism through the JAK/STAT pathway [7].

We applied the Wilcoxon algorithm to screen the hub differentially expressed transcriptional regulatory factors SIRT1 and ZNF350. Furthermore, RT-PCR and

immunofluorescence assay demonstrated that the mRNA and protein expression levels of SIRT1 and ZNF350 differed significantly between normal and OP samples in clinical studies ($n=3$), suggesting that SIRT1 and ZNF350 could considered as biomarkers for diagnosing OP. SIRT1(Silent mating type information regulation 2 homolog- 1) is a type III acetyltransferase important in the pathophysiology of metabolic diseases, degenerative diseases, cancer, and aging [32]. Studies have shown that SIRT1 expression increases in the nucleus and cytoplasm of peripheral blood mononuclear cells in patients with OP [33]. Similarly, related studies have confirmed that the specific knockout of SIRT1 in preosteoclasts has no significant effect on the volume of cancellous bone; in contrast, the specific knockout of SIRT1 in mature osteoblasts results in cancellous bone. The volume of the body is significantly reduced, and the activation or overexpression of SIRT1 reduces bone loss due to age [34–36].

SIRT1, with diverse roles in bone biology, is central to various cellular processes. Louvet et al. linked SIRT1 to bone mass in OP. In the separation-based anorexia (SBA) mouse model, activating SIRT1 reduced adipogenesis of BMSCs and increased osteogenesis, while inhibition had opposite effects. Resveratrol restored SIRT1 levels, which normalized bone parameters. These findings, seen through acetylation levels of transcription factors Runx2 and Foxo1 [37], underscore SIRT1's intricate interplay in bone health.

Moreover, SIRT1, a prominent cellular regulator, is a sensor of cellular energy and metabolism [38]. Evidence supports its involvement in endocrine and metabolic disorders, notably OP [39]. Observations indicate SIRT1 influences bone remodeling through intricate signaling pathways, including the somatotropic axis [40]. The potential association with steroid hormone signaling is substantiated by upregulated SIRT1 expression upon estrogen treatment. Conversely, ovariectomy (OVX) induces a decline in SIRT1 expression [41].

SIRT1 plays a pivotal role in epigenetic regulation of bone physiology. Nutrients impact metabolic processes [42], contributing to SIRT1's role in orchestrating tissue homeostasis through protein deacetylation [43]. Research suggests age-related pathologies, including OP, could be mitigated by modulating adipose mobilization, myogenic differentiation, dietary intake, and overall metabolism [44]. This interconnected understanding emphasizes SIRT1's multifaceted impact on bone health and its potential therapeutic relevance.

ZNF350, also known as zinc-finger 350, participates in cell proliferation during the development of various diseases, such as breast, colon, and cervical cancers [45–47]. ZNF350 also acts as a transcriptional corepressor, inhibits the expression of SNAI2, and regulates epithelial mediator transformation (EMT)-associated genes such as MMP9, KAP1, and SNAI2, thereby inhibiting tumor EMT [48].

Research suggests that ZNF350 plays a role in the pathogenesis of diseases through involvement in ferroptosis. ZNF350 forms a transcription factor complex by binding with IRF1. It directly associates with the GPX4 promoter region, suppressing GPX4 transcription and inducing ferroptosis [49]. Moreover, ZNF350, by regulating NCOA4 transcription, modulates iron accumulation, lipid peroxidation, and ferroptosis, thereby influencing glioma progression [50]. Additionally, ZNF350 typically functions as a monomer, impacting the transcription of downstream genes. For example, ZNF350 impedes cervical cancer progression by directly binding to the MMP9 promoter region and inhibiting its transcription [47]. Nevertheless, the role of ZNF350 in bone homeostasis has not been thoroughly investigated.

Our investigation has identified and substantiated ZNF350 as a diagnostic biomarker for OP. The prospective trajectory of our research will center on meticulous validation across diverse sample cohorts and the implementation of a multi-method approach. Additionally, our focus will extend to elucidating the intricate mechanistic aspects underpinning the diagnostic efficacy of ZNF350. This holistic strategy is poised to deepen our comprehension of OP and pave the way for the development of more refined and effective diagnostic methodologies. Nevertheless, this study's limitations include its reliance on the small sample size of the GSE56814 dataset and clinical verification research, which such constraints may introduce bias and restrict the representation of the target population. Thus, it is imperative to conduct further clinical experiments to validate these findings in the future, and our team remains committed to monitoring this research closely.

Conclusion

We identified key transcriptional regulators and pathways associated with OP occurrence and development through a series of comprehensive bioinformatics analyses. The identified transcriptional regulators included SIRT1 and ZNF350, which can serve as potential biomarkers for the diagnosis and prognosis of OP and will be further validated in further studies.

Abbreviations

BP	Biological processes
CC	Cellular components
FC	Fold change
FGF23	Fibroblast growth factor 23
GEO	Gene Expression Omnibus
Gly	Glycyrrhizic acid

GO	Gene Ontology
GSVA	Gene set variation analysis
IL-6	Interleukin 6
KEGG	Kyoto Encyclopedia of Genes and Genomes
ME	Module eigengene
MF	Molecular function
MM	Modular association
OP	Osteoporosis
RANK	Receptor activator of nuclear factor (NF)-κB
RT-qPCR	Reverse-transcription quantitative polymerase chain reaction
SIRT1	Silent mating type information regulation 2 homolog- 1
TNFR	Tumor necrosis factor receptor
TOM	Topological overlap matrix
WGCNA	Weighted gene co-expression network analysis
ZNF350	Zinc-finger 350

Supplementary Information The online version contains supplementary material available at https://doi.org/10.1007/s11033-024-09406-8.

Acknowledgements We would like to thank Editage (www.editage.com) for English language editing.

Author contributions [Xu, Wei] and [Liguo, Zhu] contributed to the study conception and design. Material preparation, data collection and analysis were performed by [Jingyi, Hou], [Jingyuan, Si], [Bin Chen]. The experimental validation was performed by [Ning, Yang]. The first draft of the manuscript was written by [Naiqiang, Zhu] and all authors commented on previous versions of the manuscript. All authors read and approved the final manuscript.

Funding This work was supported by the Medical Science Research Project Program of Hebei Provincial Health Commission (No. 20210121) ;Hebei Natural Science Foundation (H2022406038). National Natural Science Foundation of China (82305055).

Data availability All the raw data used in this study are available in the public GEO database (https://www.ncbi.nlm.nih.gov/geo/). All data generated or analyzed during this study are included in this published article. The datasets generated during and/or analyzed during the current study are available from the corresponding author on reasonable request.

Declarations

Ethics approval Three osteoporotic bone tissues were obtained from patients with osteoporotic fracture surgery. Three normal bone tissues were obtained from patients with traumatic amputation. This study was performed in line with the principles of the Declaration of Helsinki. Approval was granted by the Ethics Committee of The Affiliated Hospital of Chengde Medical University (2022.06.16/ No. CYFYLL2020240).

Consent to participate Informed consent was obtained from all individual participants included in the study.

Consent to publish The authors affirm that human research participants provided informed consent for publication of the images in this article.

Conflicts of interest This study does not increase the medical costs and suffering of the subjects, and research materials and research results are used for scientific purposes without a conflict of interest.

References

1. Srivastava M, Deal C (2002) Osteoporosis in elderly: prevention and treatment. Clin Geriatr Med 18:529–555. https://doi.org/10.1016/s0749-0690(02)00022-8
2. Link TM, Majumdar S (2003) Osteoporosis imaging. Radiol Clin North Am 41:813–839. https://doi.org/10.1016/s0033-8389(03)00059-9
3. Straka M, Straka-Trapezanlidis M, Deglovic J, Varga I (2015) Periodontitis and osteoporosis. Neuro Endocrinol Lett 36:401–406
4. Bijelic R, Milicevic S, Balaban J (2017) Risk factors for osteoporosis in Postmenopausal Women. Med Arch 71:25–28. https://doi.org/10.5455/medarh.2017.71.25-28
5. Feng Y, Wan P, Yin L, Lou X (2020) The inhibition of MicroRNA-139-5p promoted osteoporosis of bone marrow-derived mesenchymal stem cells by targeting Wnt/Beta-Catenin signaling pathway by NOTCH1. J Microbiol Biotechnol 30:448–458. https://doi.org/10.4014/jmb.1908.08036
6. Wang CG, Hu YH, Su SL, Zhong D (2020) LncRNA DANCR and miR-320a suppressed osteogenic differentiation in osteoporosis by directly inhibiting the Wnt/beta-catenin signaling pathway. Exp Mol Med 52:1310–1325. https://doi.org/10.1038/s12276-020-0475-0
7. Xu L, Zhang L, Zhang H et al (2018) The participation of fibroblast growth factor 23 (FGF23) in the progression of osteoporosis via JAK/STAT pathway. J Cell Biochem 119:3819–3828. https://doi.org/10.1002/jcb.26332
8. Damerau A, Gaber T, Ohrndorf S, Hoff P (2020) JAK/STAT activation: a general mechanism for Bone Development, Homeostasis, and regeneration. Int J Mol Sci 21. https://doi.org/10.3390/ijms21239004
9. Wang XL, Liu YM, Zhang ZD et al (2020) Utilizing benchmarked dataset and gene regulatory network to investigate hub genes in postmenopausal osteoporosis. J Cancer Res Ther 16:867–873. https://doi.org/10.4103/0973-1482.204842
10. Yang Z, Zi Q, Xu K et al (2021) Development of a macrophages-related 4-gene signature and nomogram for the overall survival prediction of hepatocellular carcinoma based on WGCNA and LASSO algorithm. Int Immunopharmacol 90:107238. https://doi.org/10.1016/j.intimp.2020.107238
11. Tian Z, He W, Tang J et al (2020) Identification of important modules and biomarkers in breast Cancer based on WGCNA. Onco Targets Ther 13:6805–6817. https://doi.org/10.2147/OTT.S258439
12. Feng T, Li K, Zheng P et al (2019) Weighted Gene Coexpression Network Analysis Identified MicroRNA Coexpression Modules and Related Pathways in Type 2 Diabetes Mellitus. Oxid Med Cell Longev 2019:9567641. https://doi.org/10.1155/2019/9567641
13. Rangaraju S, Dammer EB, Raza SA et al (2018) Identification and therapeutic modulation of a pro-inflammatory subset of disease-associated-microglia in Alzheimer's disease. Mol Neurodegener 13:24. https://doi.org/10.1186/s13024-018-0254-8
14. Tang Y, Ke ZP, Peng YG, Cai PT (2018) Co-expression analysis reveals key gene modules and pathway of human coronary heart disease. J Cell Biochem 119:2102–2109. https://doi.org/10.1002/jcb.26372

15. Xia B, Li Y, Zhou J et al (2017) Identification of potential pathogenic genes associated with osteoporosis. Bone Joint Res 6:640–648. https://doi.org/10.1302/2046-3758.612.BJR-2017-0102.R1
16. Langfelder P, Horvath S (2008) WGCNA: an R package for weighted correlation network analysis. BMC Bioinformatics 9:559. https://doi.org/10.1186/1471-2105-9-559
17. Zhou RH, Chen C, Jin SH et al (2020) Co-expression gene modules involved in cisplatin-induced peripheral neuropathy according to sensitivity, status, and severity. J Peripher Nerv Syst 25:366–376. https://doi.org/10.1111/jns.12407
18. Han H, Shim H, Shin D et al (2015) TRRUST: a reference database of human transcriptional regulatory interactions. Sci Rep 5:11432. https://doi.org/10.1038/srep11432
19. Han H, Cho JW, Lee S et al (2018) TRRUST v2: an expanded reference database of human and mouse transcriptional regulatory interactions. Nucleic Acids Res 46:D380–D386. https://doi.org/10.1093/nar/gkx1013
20. Yu G, Wang LG, Han Y, He QY (2012) clusterProfiler: an R package for comparing biological themes among gene clusters. OMICS 16:284–287. https://doi.org/10.1089/omi.2011.0118
21. Hänzelmann S, Castelo R, Guinney J (2013) GSVA: gene set variation analysis for microarray and RNA-seq data. BMC Bioinformatics 14:7. https://doi.org/10.1186/1471-2105-14-7
22. Wang Z, Wang D, Liu Y et al (2021) Mesenchymal stem cell in mice uterine and its therapeutic effect on osteoporosis. Rejuvenation Res 24:139–150. https://doi.org/10.1089/rej.2019.2262
23. Miller PD (2016) Management of severe osteoporosis. Expert Opin Pharmacother 17:473–488. https://doi.org/10.1517/14656566.2016.1124856
24. Kaliman P, Vinals F, Testar X et al (1996) Phosphatidylinositol 3-kinase inhibitors block differentiation of skeletal muscle cells. J Biol Chem 271:19146–19151. https://doi.org/10.1074/jbc.271.32.19146
25. Sakaue H, Ogawa W, Matsumoto M et al (1998) Posttranscriptional control of adipocyte differentiation through activation of phosphoinositide 3-kinase. J Biol Chem 273:28945–28952. https://doi.org/10.1074/jbc.273.44.28945
26. Ghosh-Choudhury N, Abboud SL, Nishimura R et al (2002) Requirement of BMP-2-induced phosphatidylinositol 3-kinase and akt serine/threonine kinase in osteoblast differentiation and smad-dependent BMP-2 gene transcription. J Biol Chem 277:33361–33368. https://doi.org/10.1074/jbc.M205053200
27. Xi JC, Zang HY, Guo LX et al (2015) The PI3K/AKT cell signaling pathway is involved in regulation of osteoporosis. J Recept Signal Transduct Res 35:640–645. https://doi.org/10.3109/10799893.2015.1041647
28. Asagiri M, Takayanagi H (2007) The molecular understanding of osteoclast differentiation. Bone 40:251–264. https://doi.org/10.1016/j.bone.2006.09.023
29. Cao B, Dai X, Wang W (2019) Knockdown of TRPV4 suppresses osteoclast differentiation and osteoporosis by inhibiting autophagy through ca(2+) -calcineurin-NFATc1 pathway. J Cell Physiol 234:6831–6841. https://doi.org/10.1002/jcp.27432
30. Yin Z, Zhu W, Wu Q et al (2019) Glycyrrhizic acid suppresses osteoclast differentiation and postmenopausal osteoporosis by modulating the NF-kappaB, ERK, and JNK signaling pathways. Eur J Pharmacol 859:172550. https://doi.org/10.1016/j.ejphar.2019.172550
31. Zi Z, Cho KH, Sung MH et al (2005) In silico identification of the key components and steps in IFN-gamma induced JAK-STAT signaling pathway. FEBS Lett 579:1101–1108. https://doi.org/10.1016/j.febslet.2005.01.009
32. Carafa V, Nebbioso A, Altucci L (2012) Sirtuins and disease: the road ahead. Front Pharmacol 3:4. https://doi.org/10.3389/fphar.2012.00004
33. Godfrin-Valnet M, Khan KA, Guillot X et al (2014) Sirtuin 1 activity in peripheral blood mononuclear cells of patients with osteoporosis. Med Sci Monit Basic Res 20:142–145. https://doi.org/10.12659/MSMBR.891372
34. Simic P, Zainabadi K, Bell E et al (2013) SIRT1 regulates differentiation of mesenchymal stem cells by deacetylating beta-catenin. EMBO Mol Med 5:430–440. https://doi.org/10.1002/emmm.201201606
35. Edwards JR, Perrien DS, Fleming N et al (2013) Silent information regulator (Sir)T1 inhibits NF-kappaB signaling to maintain normal skeletal remodeling. J Bone Min Res 28:960–969. https://doi.org/10.1002/jbmr.1824
36. Mercken EM, Mitchell SJ, Martin-Montalvo A et al (2014) SRT2104 extends survival of male mice on a standard diet and preserves bone and muscle mass. Aging Cell 13:787–796. https://doi.org/10.1111/acel.12220
37. Louvet L, Leterme D, Delplace S et al (2020) Sirtuin 1 deficiency decreases bone mass and increases bone marrow adiposity in a mouse model of chronic energy deficiency. Bone 136:115361. https://doi.org/10.1016/j.bone.2020.115361
38. Ke L, Li Q, Song J et al (2021) The mitochondrial biogenesis signaling pathway is a potential therapeutic target for myasthenia gravis via energy metabolism (review). Exp Ther Med 22:702. https://doi.org/10.3892/etm.2021.10134
39. Lu C, Zhao H, Liu Y et al (2023) Novel role of the SIRT1 in endocrine and metabolic diseases. Int J Biol Sci 19:484–501. https://doi.org/10.7150/ijbs.78654
40. Toorie AM, Cyr NE, Steger JS et al (2016) The nutrient and energy sensor Sirt1 regulates the hypothalamic-pituitary-adrenal (HPA) Axis by altering the production of the Prohormone Convertase 2 (PC2) essential in the maturation of corticotropin-releasing hormone (CRH) from its prohormone in male rats. J Biol Chem 291:5844–5859. https://doi.org/10.1074/jbc.M115.675264
41. Wang X, Chen L, Peng W (2017) Protective effects of resveratrol on osteoporosis via activation of the SIRT1-NF-κB signaling pathway in rats. Exp Ther Med 14:5032–5038. https://doi.org/10.3892/etm.2017.5147
42. Tozzi R, Cipriani F, Masi D et al (2022) Ketone bodies and SIRT1, Synergic Epigenetic Regulators for Metabolic Health: a narrative review. Nutrients 14:3145. https://doi.org/10.3390/nu14153145
43. Nakagawa T, Guarente L (2011) Sirtuins at a glance. J Cell Sci 124:833–838. https://doi.org/10.1242/jcs.081067
44. Cohen-Kfir E, Artsi H, Levin A et al (2011) Sirt1 is a regulator of bone mass and a repressor of Sost encoding for sclerostin, a bone formation inhibitor. Endocrinology 152:4514–4524. https://doi.org/2020071613282569900
45. Garcia V, Dominguez G, Garcia JM et al (2004) Altered expression of the ZBRK1 gene in human breast carcinomas. J Pathol 202:224–232. https://doi.org/10.1002/path.1513
46. Garcia V, Garcia JM, Pena C et al (2005) The GADD45, ZBRK1 and BRCA1 pathway: quantitative analysis of mRNA expression in colon carcinomas. J Pathol 206:92–99. https://doi.org/10.1002/path.1751
47. Lin LF, Chuang CH, Li CF et al (2010) ZBRK1 acts as a metastatic suppressor by directly regulating MMP9 in cervical cancer. Cancer Res 70:192–201. https://doi.org/10.1158/0008-5472.CAN-09-2641
48. Patnaik S, George SP, Pham E et al (2016) By moonlighting in the nucleus, villin regulates epithelial plasticity. Mol Biol Cell 27:535–548. https://doi.org/10.1091/mbc.E15-06-0453
49. Zhang Y, Zhang J, Feng D et al (2022) IRF1/ZNF350/GPX4-mediated ferroptosis of renal tubular epithelial cells promote chronic renal allograft interstitial fibrosis. Free Radic Biol Med 193:579–594. https://doi.org/10.1016/j.freeradbiomed.2022.11.002
50. Lin Y, Gong H, Liu J et al (2023) HECW1 induces NCOA4-regulated ferroptosis in glioma through the ubiquitination and

degradation of ZNF350. Cell Death Dis 14:794. https://doi.org/10.1038/s41419-023-06322-w